Supporting Information

Polyoxometalate-based Well-defined rod-like Structural Mutifunctional Materials: Synthesis, Structure, Properties

Xi-Ming Luo,[†] Ning-Fang Li,[†] Zhao-Bo Hu,[‡] Jia-Peng Cao,[†] Chen-Hui Cui,[†] Qing-Fang Lin,[†] and Yan Xu[*,†,‡]*

[†]College of Chemical Engineering, State Key Laboratory of Materials-Oriented Chemical Engineering, Nanjing Tech University, Nanjing 210009, P. R. China

[‡]Coordination Chemistry Institute, State Key Laboratory of Coordination Chemistry, Nanjing University, Nanjing 210093, P. R. China

Physical Measurements

Elemental analyses (C, H and N) were performed on a Perkin-Elmer 2400 elemental analyzer.

Powder X-ray diffraction (PXRD) patterns were recorded on a Bruker D8X diffractometer equipped with monochromatized Cu-K_α (λ = 1.5418 Å) radiation at room temperature. Data were collected in the range of 5−50 °.

IR spectra of compounds **1**–**3** were recorded on a Nicolet Impact 410 FTIR spectrometer with pressed KBr pellets, from 4000 to 400 cm^{-1}.

Thermogravimetric (TG) measurements were carried out on a Diamond thermogravimetric analyzer in a flowing N_2 atmosphere from 25 to 800 °C, with a heating rate of 10 °C·min^{-1}.

Two-photon absorption (TPA) cross-sections (σ) were obtained by using a Chameleon II femtosecond laser pulse and Ti:95 sapphire system.

A CHI 760 Electrochemical workstation was used for the electrochemical experiments. A conventional three-electrode cell was used at room temperature. The complex bulk-modified carbon-paste electrode (CPE) was used as the working electrodes. An Ag/AgCl and a platinum wire were used as reference and auxiliary electrodes, respectively.

The variable temperature magnetic susceptibility data were measured over the temperature range of 1.8-300 K and the isothermal magnetization measurements were carried out between 0 and 7 T, using a Quantum Design MPMS-XL 7 SQUID magnetometer. The experimental magnetic susceptibility data for all compounds were corrected for diamagnetic contributions estimated using Pascal's constant and of the sample holder by a previous calibration.

Preparation of bulk-modified carbon paste electrode (CPE). The bulk-modified CPE was fabricated as follows. Grinding a mixture of 0.10 g graphite powder and 0.030 g of the obtained complex in an agate mortar for approximately 0.5 h produced a uniform mixture. 0.2 mL paraffin oil was then added and stirred with a glass rod. The homogenized mixture was packed into a 3 mm inner diameter glass tube and the tube surface was wiped with weighing paper. The electrical contact was established with the copper wire through the back of the electrode.

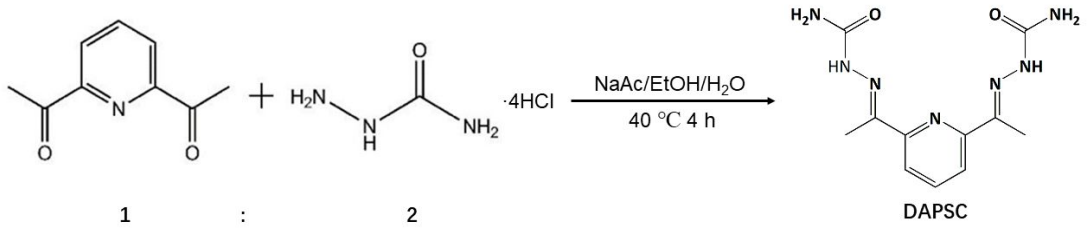

Scheme S1. Synthesis of 2,6-diacetylpyridine bis(semicarbazone) (DAPSC).

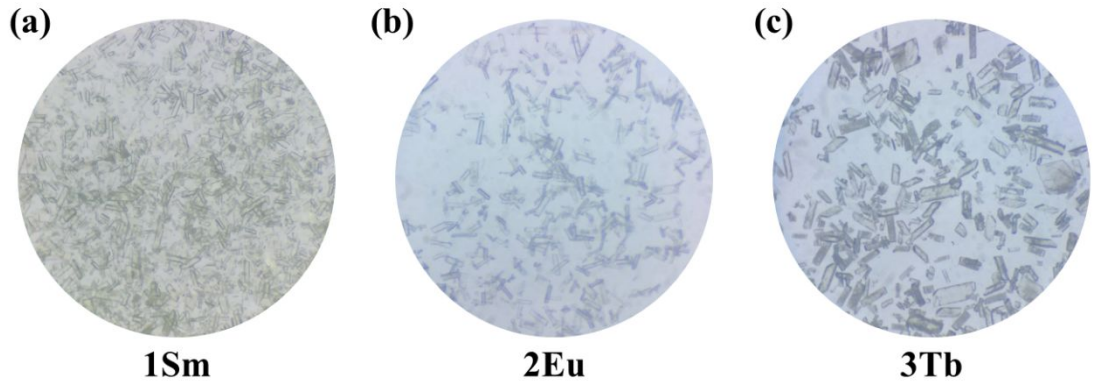

Figure S1. The images of crystals **1-3** under optical microscope.

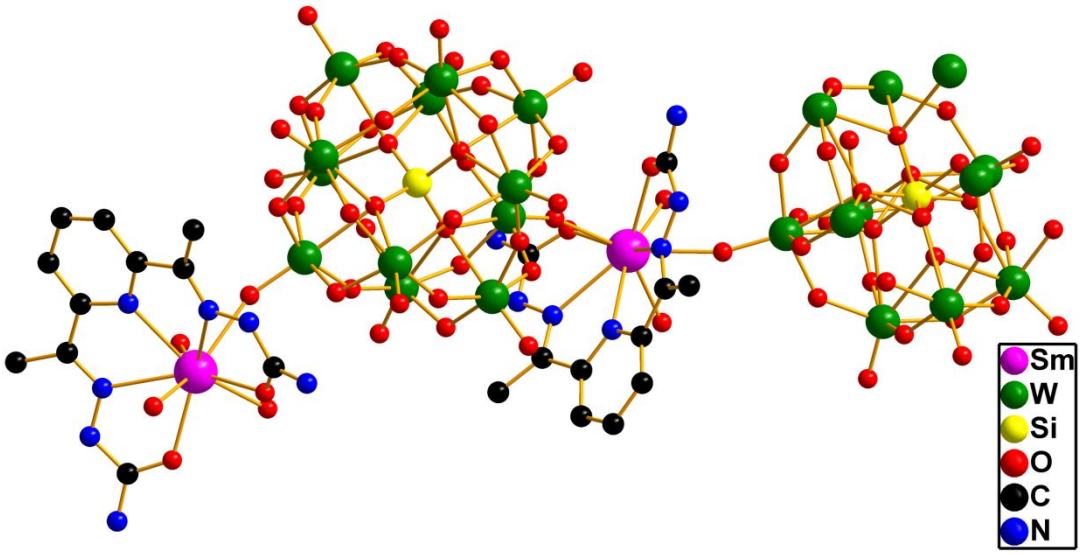

Figure S2. Ball and stick representation of the basic crystallographic unit in **1Sm**. Hydrogen atoms and crystallization water molecules are omitted for clarity.

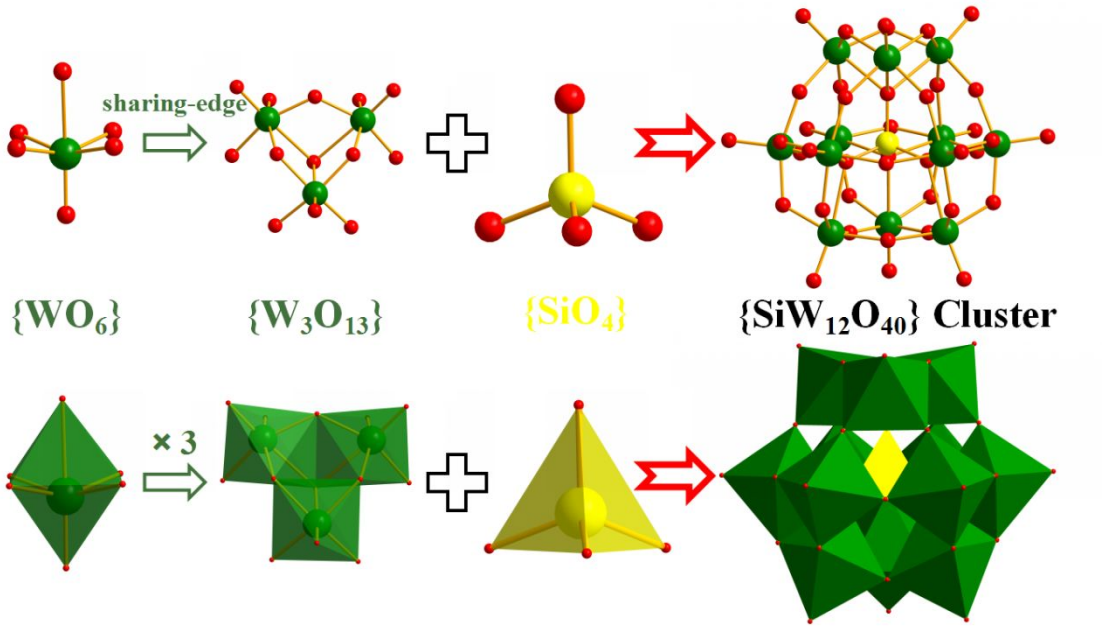

Figure S3. The structure of anion $[SiW_{12}O_{40}]^{4-}$ cluster.

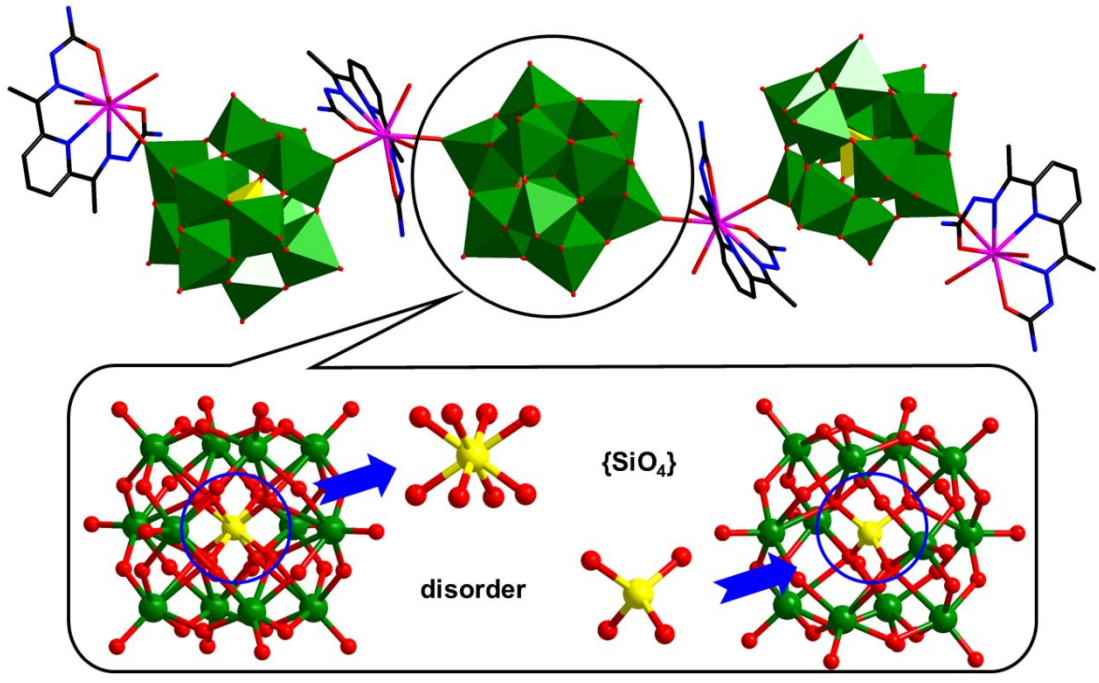

Figure S4. The disorder of $\{SiO_4\}$ in the middle POMs.

SiW_{12} can be conveniently viewed as constructed by a central tetrahedron $\{SiO_4\}$ surrounded by four triplets $\{W_3O_{13}\}$, in which three identical octahedra $\{WO_6\}$ units

are joined together by sharing edges. Twelve octahedra $\{WO_6\}$ building blocks centered around a tetrahedron $\{SiO_4\}$ are joined together by sharing of corners to produce the classical cluster. The Si-O distances of compounds fall into the ranges of 1.56(2)-1.654(19) Å and the W-O distances can be grouped into disparate sections, *eg*. W - O_t = 1.634(15) - 1.734(10) Å, W - O_b = 1.680(11) - 1.960(12) Å, and W - O_c = 2.282(11) - 2.47(2) Å.

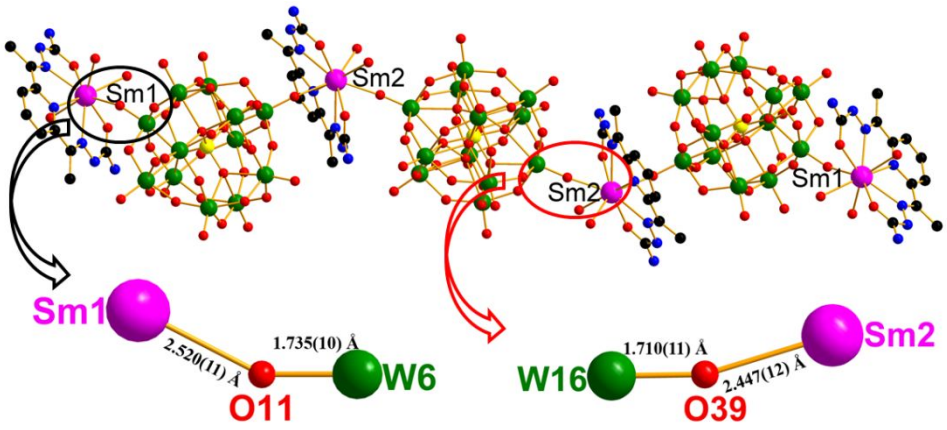

Figure S5. The special bond length of complex **1Sm**.

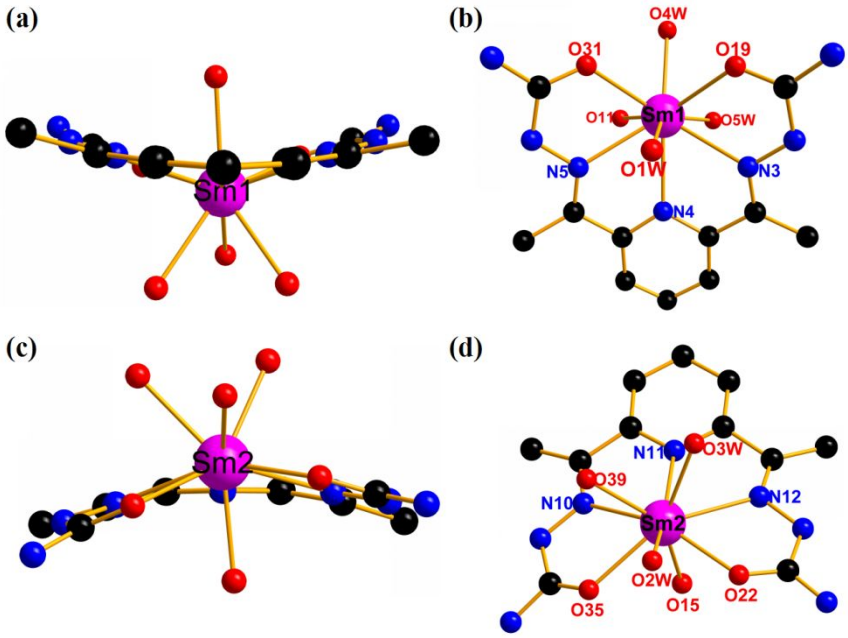

Figure S6. The rigid concave surface of Sm-L_{Schiff} complexes (Sm1, (a); Sm2, (c)); Coordination mode of two crystallographically independent Sm^{3+} centers (Sm1, (b); Sm2, (d)) in **1Sm**. Hydrogens are omitted for clarity.

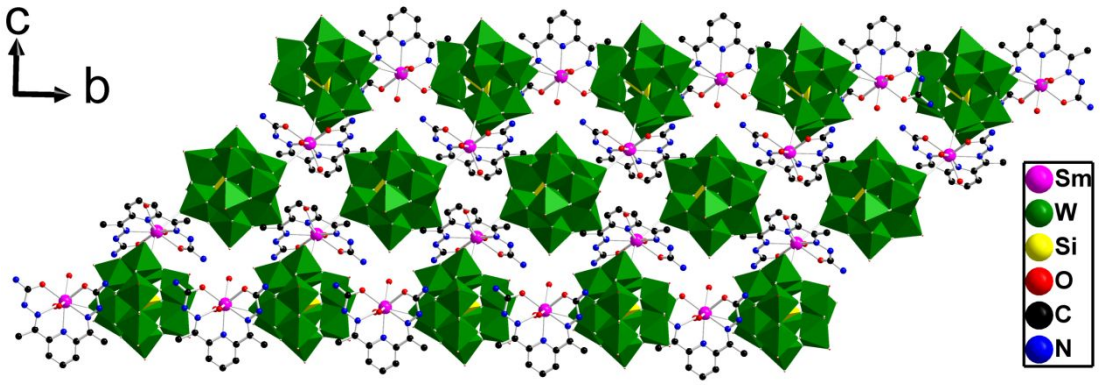

Figure S7. The 3D supramolecular structure of **1Sm** along the *a*-axis. The hydrogen atoms and crystallization water molecules are omitted for clarity.

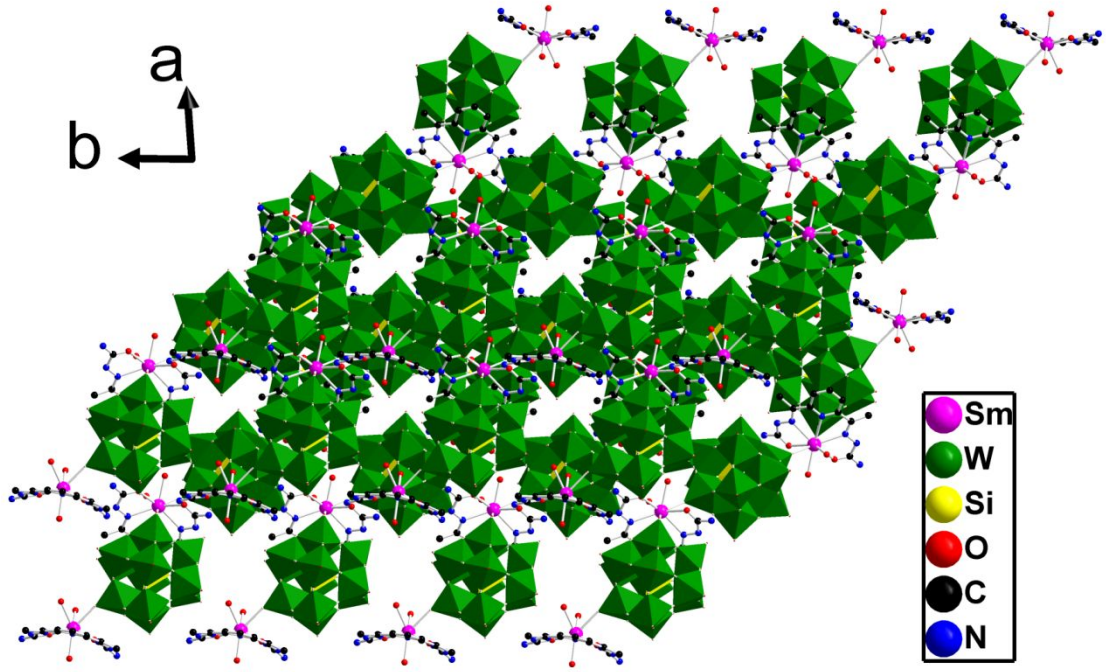

Figure S8. The 3D supramolecular structure of **1Sm** along the *c*-axis. The hydrogen atoms and crystallization water molecules are omitted for clarity.

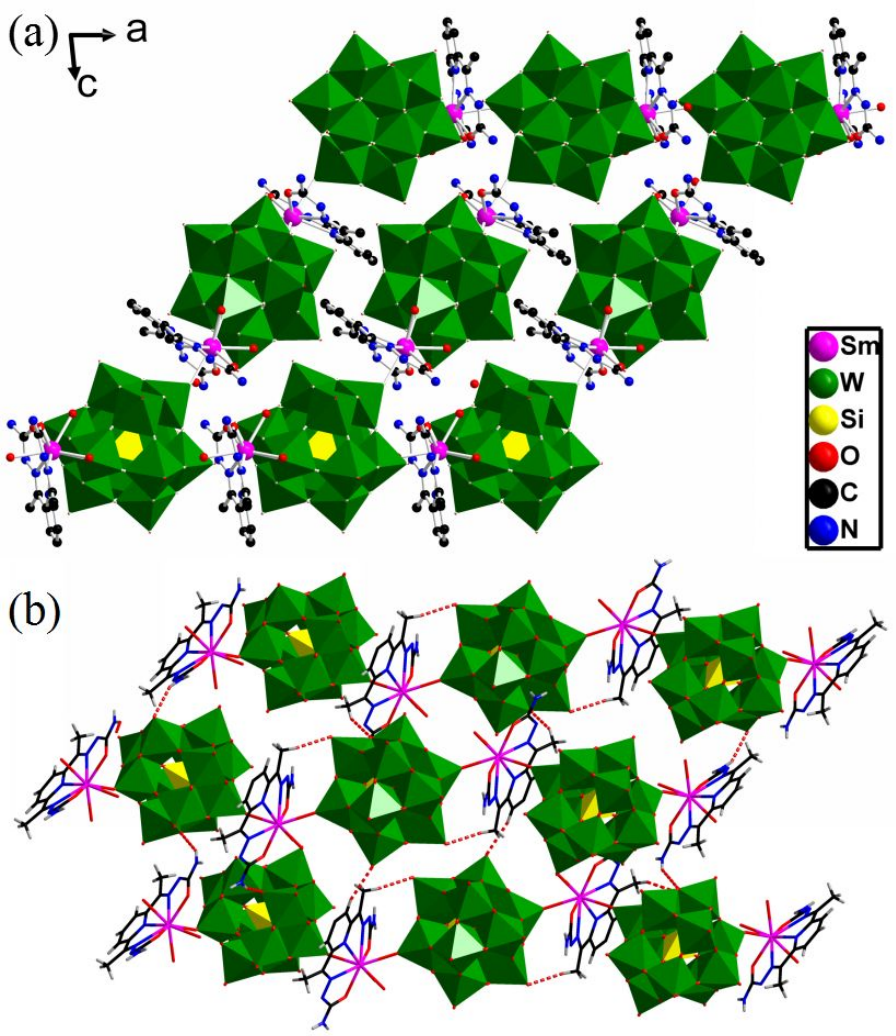

Figure S9. (a) The 3D supramolecular structure of **1Sm**. (b) The hydrogen bonding interactions in **1Sm**.

XRD

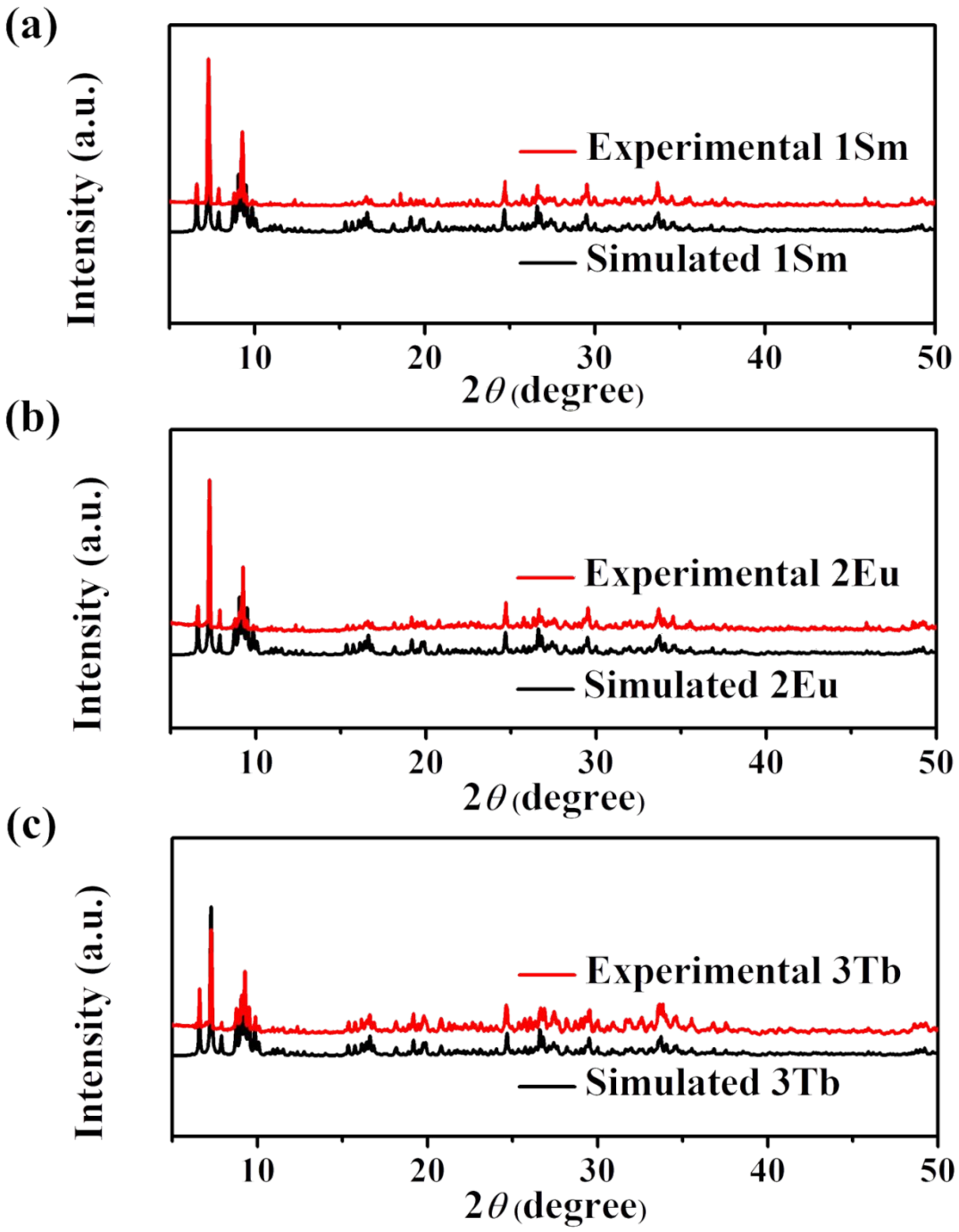

Figure S10. PXRD patterns of all compounds **1-3**.

Powder X-ray diffraction. PXRD measurements for **1-3** were undertaken at room temperature. The experimental and simulated XRD patterns of **1-3** are shown in Figure 3a and Figure S10. The PXRD patterns of **1**−**3** are almost the same and match well with the simulated pattern obtained from X-ray single-crystal data. The difference in reflection intensities between the simulated and the experimental

patterns is due to the different orientation of the crystals in the powder samples. No other peaks being found in the pattern revealed that the product has no impurities.

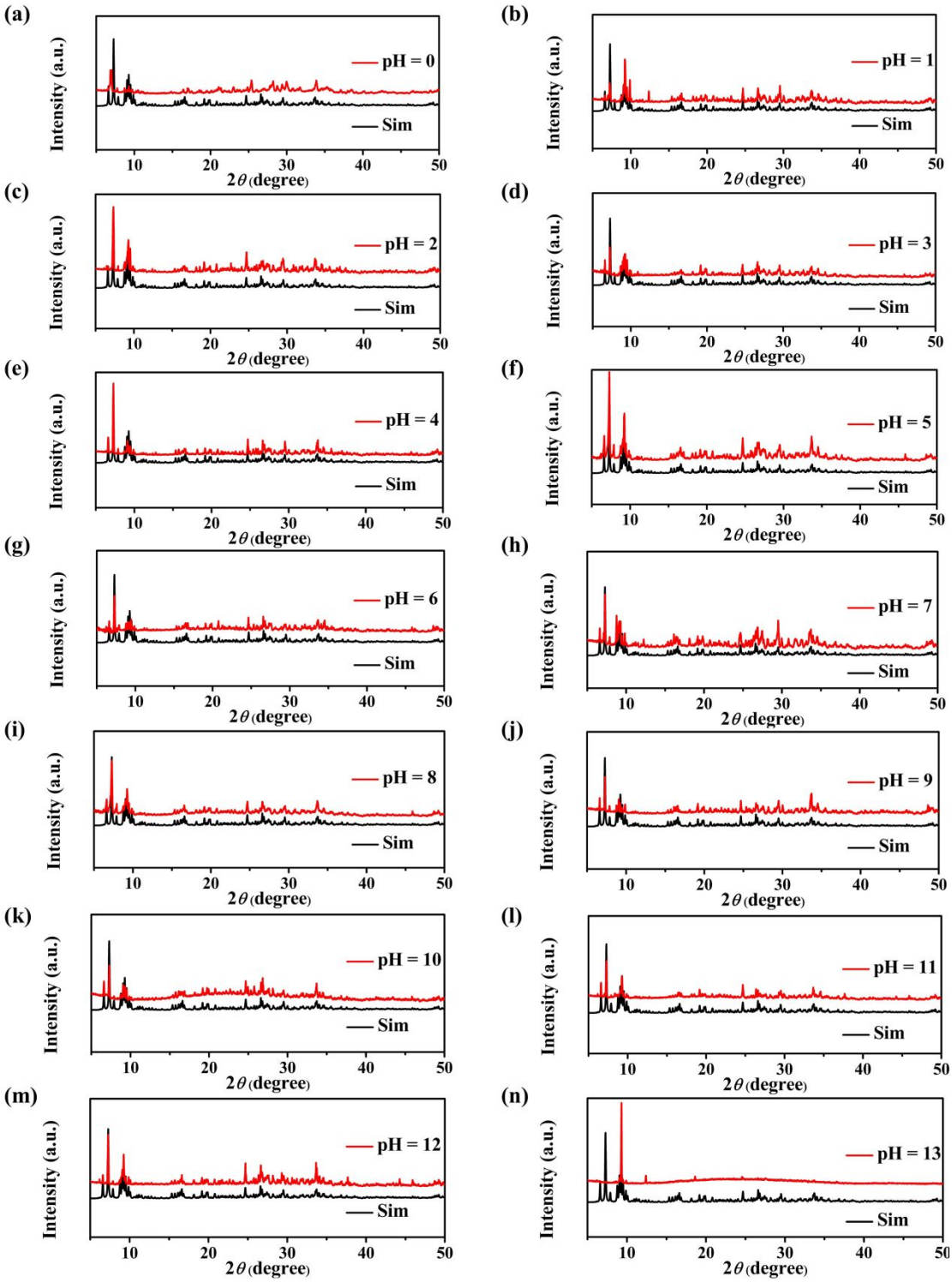

Figure S11. Variable-pH PXRD of **2Eu**.

IR

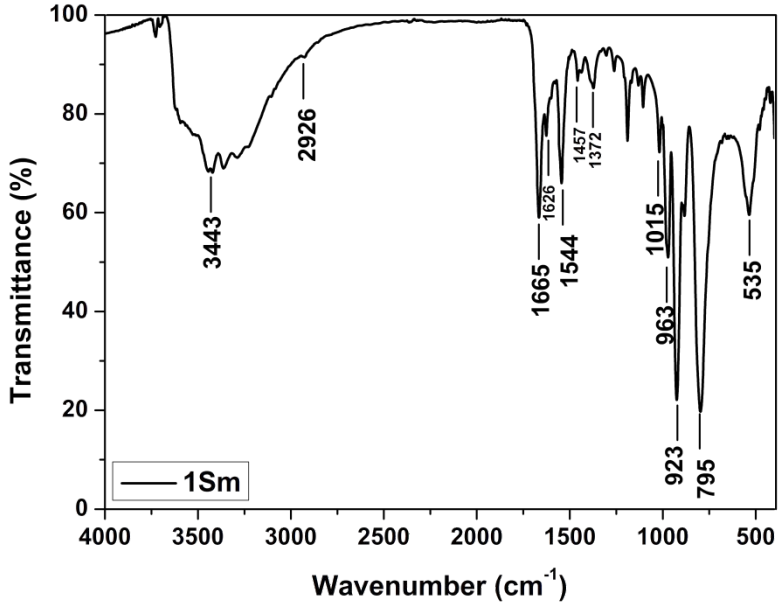

Figure S12. FT-IR spectra of **1Sm**.

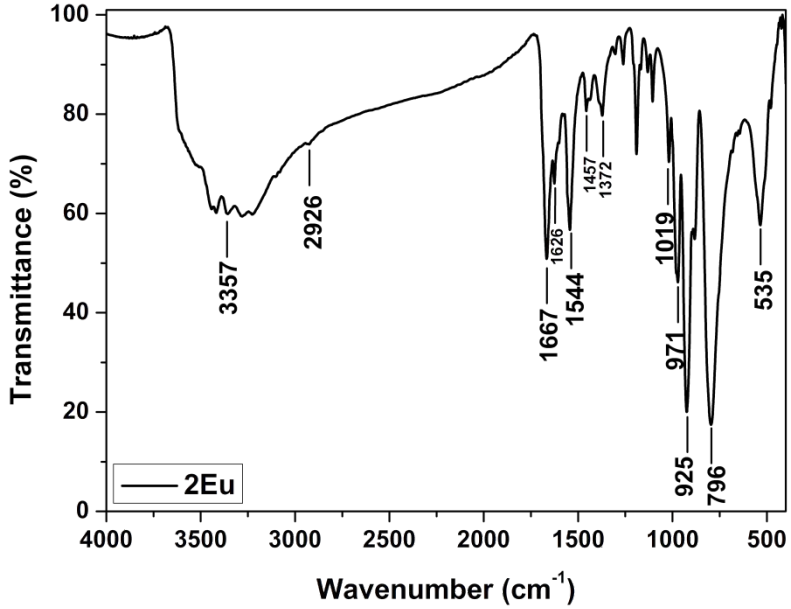

Figure S13. FT-IR spectra of **2Eu**.

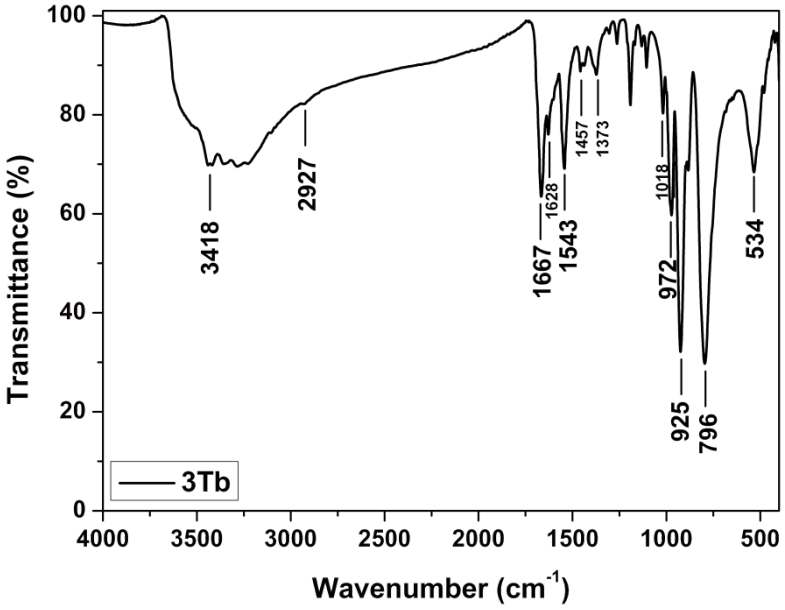

Figure S14. FT-IR spectra of **3Tb**.

TG

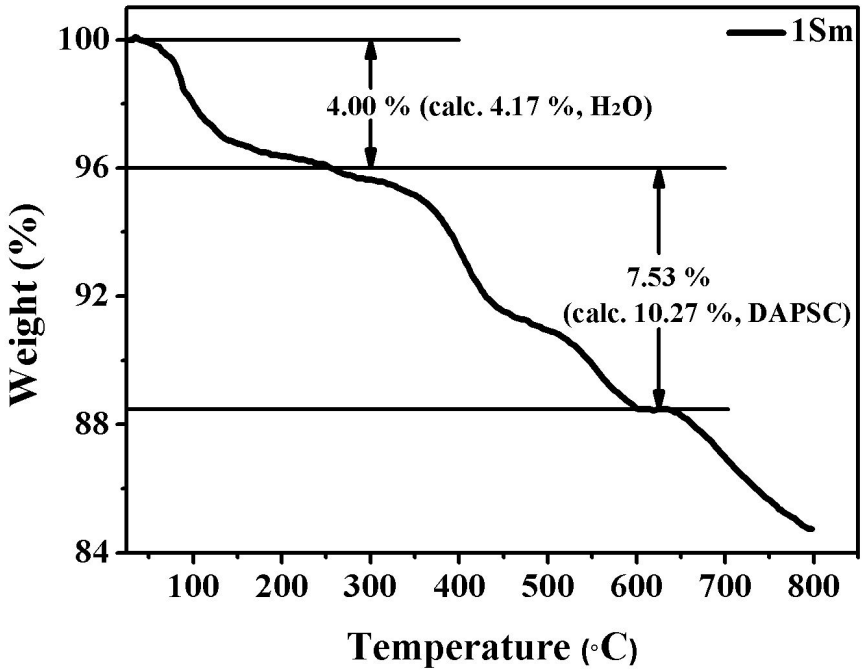

Figure S15. TG curve of **1Sm**.

1Sm lose a mass of 7.53 %, which situates in range (250-625 °C). It is attributed to the thermal decomposition of organic constituent. The difference between the test and theoretical values (10.27 %) may be due to carbon residues on the surface of the material.

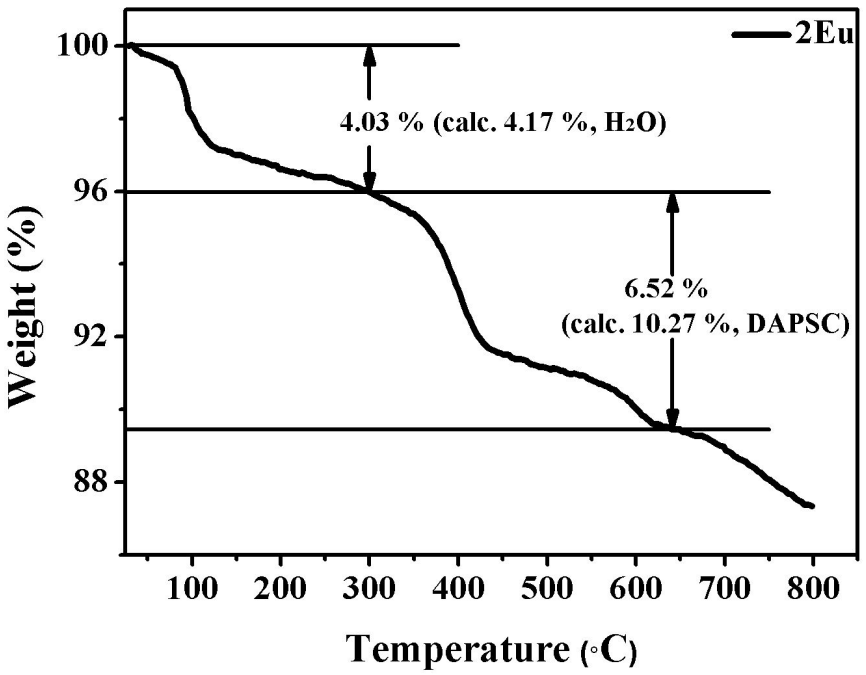

Figure S16. TG curve of **2Eu**.

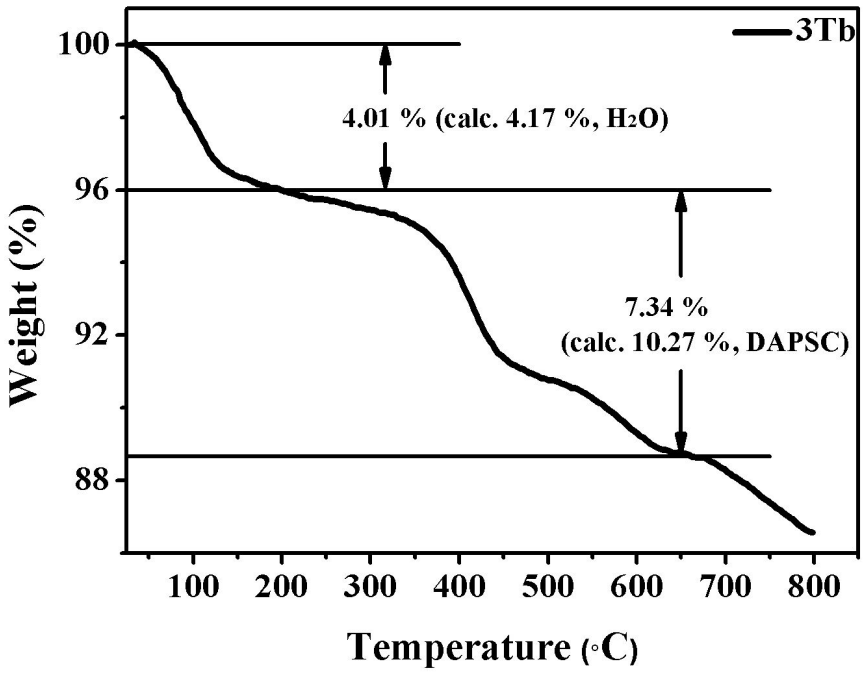

Figure S17. TG curve of **3Tb**.

Electrochemical properties.

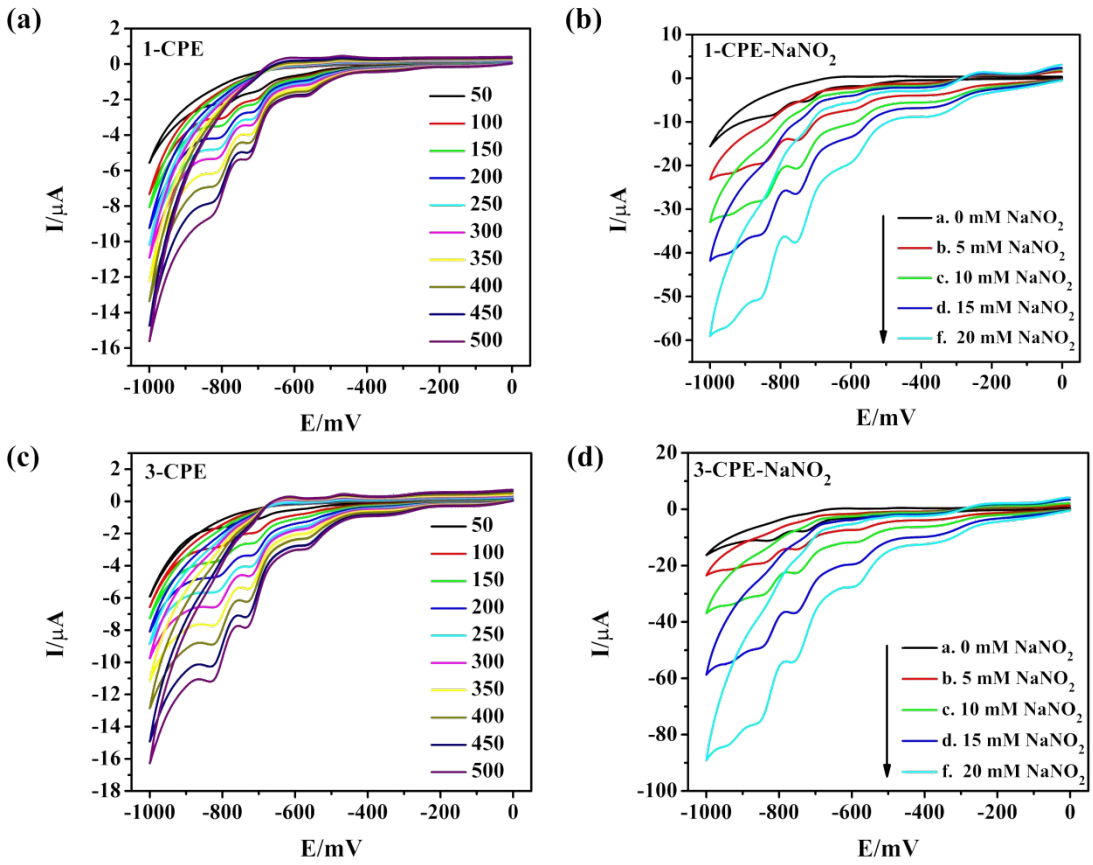

Figure 18. (a, c) Cyclic voltammograms of **1-CPE** and **3-CPE**. Solution: aqueous solution with 0.1 *M* H_2SO_4 + 0.5 *M* Na_2SO_4; Scan rates: 50-500 mV s^{-1}; (b, d) Cyclic voltammograms of **1-CPE** and **3-CPE**. Solution: 0.1 *M* H_2SO_4 + 0.5 *M* Na_2SO_4 containing 0.0–20.0 mM $NaNO_2$ (scan rates: 500 mV s^{-1}).

Nonlinear Optical properties.

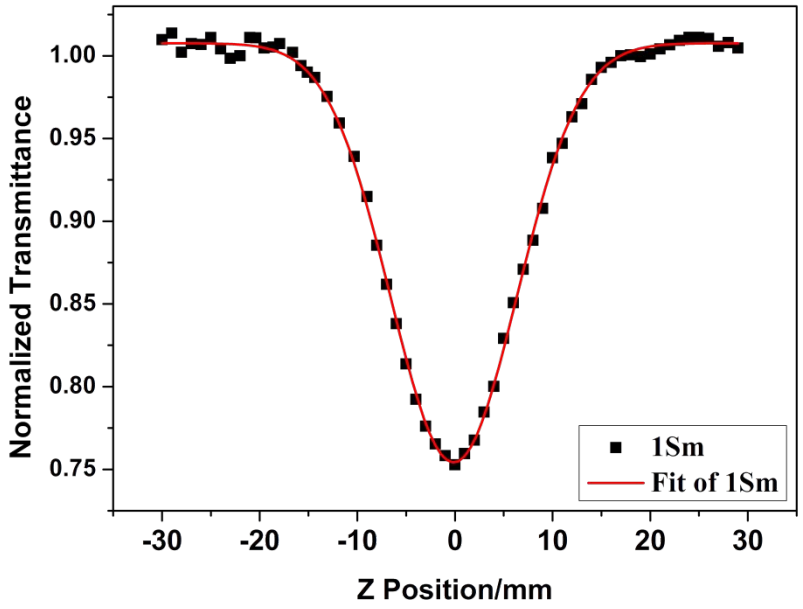

Figure S19. The open aperture Z-scan data at 680 nm for **1Sm** in DMF at 1.0×10^{-4} mol L^{-1}. The dots are the experimental data and the solid curve represent the theoretical data.

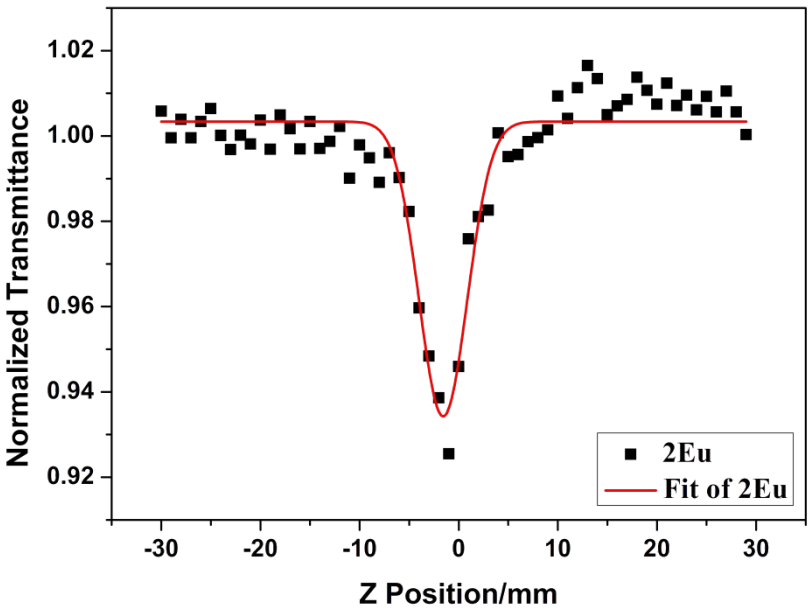

Figure S20. The open aperture Z-scan data at 700 nm for **2Eu** in DMF at 1.0×10^{-4} mol L^{-1}. The dots are the experimental data and the solid curve represent the theoretical data.

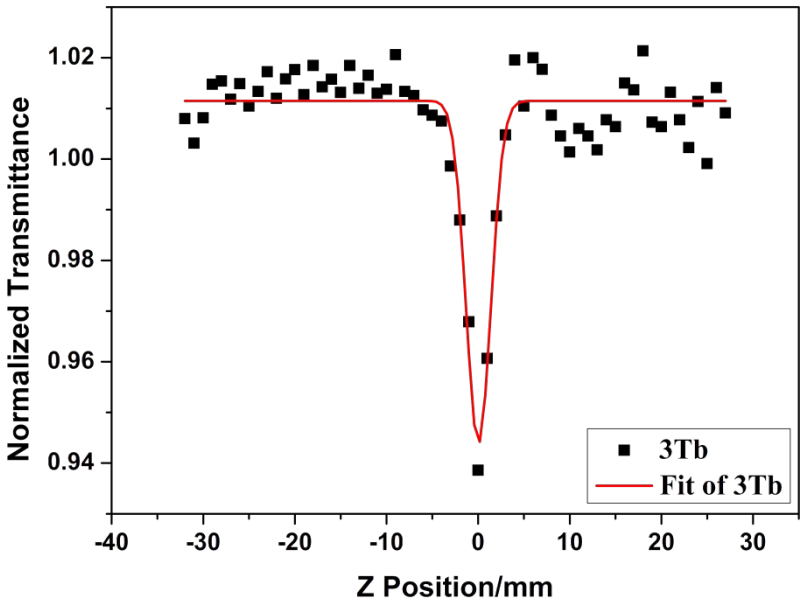

Figure S21. The open aperture Z-scan data at 720 nm for **3Tb** in DMF at 1.0×10^{-4} mol L^{-1}. The dots are the experimental data and the solid curve represent the theoretical data.

The electronic spectra of compounds **1-3** in DMF at a concentration of 1.0×10^{-4} mol L^{-1} give the nonlinear absorption at room temperature. Two-photon absorption (TPA) values containing TPA coefficient β and TPA cross section σ were measured by the open-aperture Z-scan technique with femtosecond laser pulse and Ti:95 sapphire system. Figure S19-S21 shows the open aperture Z-scan curves of compound **1-3**. The black dots are the experimental data, and the red lines represent the theoretical simulated curves modified by the following equations (eqn (1) and (2)):

$$T(z,s=1)=\sum_{m=0}^{\infty}\frac{[-q_0(z)]^m}{(m+1)^{3/2}} \quad \text{for} \quad |q_0|<1 \tag{1}$$

$$q_0(z)=\frac{\beta I_0 L_{eff}}{1+z^2/z_0^2} \tag{2}$$

where β is the TPA coefficient of the solution, I_0 is the input intensity of laser beam at the focus $z = 0$, $L_{eff} = (1\text{-}e^{-\alpha L})/\alpha$ is the effective length with α and L are the linear absorption coefficient and the sample length respectively. Z is the sample position, $z_0 = \pi\omega_0^2/\lambda$ is the diffraction length of the beam, in which the ω_0 and λ are the spot size at the focus and the wavelength of the beam respectively. Furthermore, the molecular TPA cross section σ can be calculated by the following relationship:

$$\sigma N_A d\times10^{-3}=h\nu\beta \tag{3}$$

where N_A, d, h and ν are respectively the Avogadro's constant, the concentration of the compound, the Planck's constant and the frequency of input intensity.

Magnetic properties.

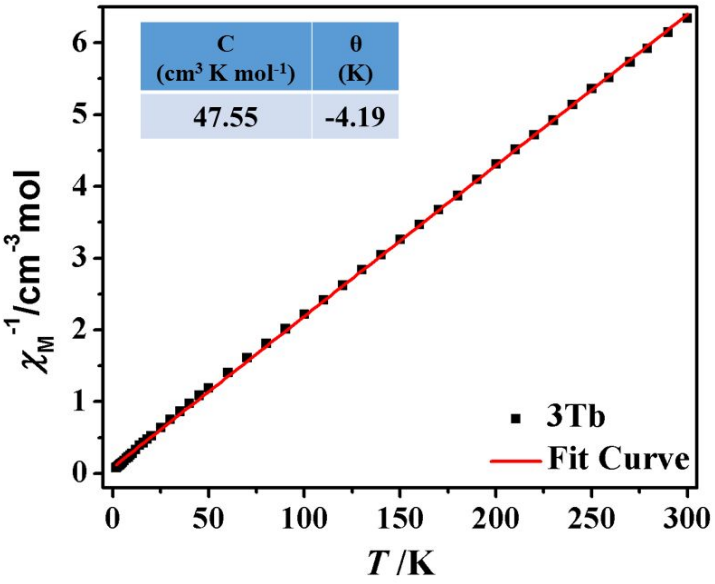

Figure S22. χ_M^{-1} versus T plot of **3Tb**. The red line is fitting result with χ_M = C /(T-θ).

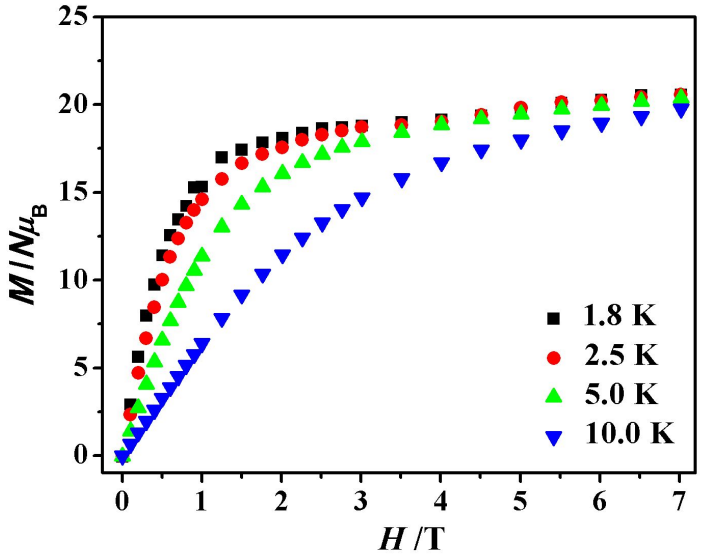

Figure S23. The isothermal field-dependence magnetization (*M*-*H*) at low temperatures for **3Tb** (1.8-10.0 K).

Table S1. Selected bond lengths (Å) for coordination environments of the two Sm^{III} ions in **1Sm**.

Sm(1)-O(31)	2.391(12)	Sm(2)-O(22)	2.392(12)	Sm(1)-N(4)	2.540(15)
Sm(1)-O(19)	2.434(11)	Sm(2)-O(15)	2.407(12)	Sm(1)-N(5)	2.555(12)
Sm(1)-O(1W)	2.452(13)	Sm(2)-O(3W)	2.443(12)	Sm(1)-N(3)	2.562(14)
Sm(1)-O(5W)	2.454(11)	Sm(2)-O(39)	2.447(12)	Sm(2)-N(10)	2.602(14)
Sm(1)-O(4W)	2.479(13)	Sm(2)-O(35)	2.457(11)	Sm(2)-N(12)	2.622(14)
Sm(1)-O(11)	2.520(11)	Sm(2)-O(2W)	2.480(13)	Sm(2)-N(11)	2.640(15)

Table S2. The selected bond lengths (Å) and bond angles (°) for **1Sm**.

W(8)-O(47)	1.665(12)	W(6)-O(25)	1.916(11)	W(14)-O(51)^{i}	1.877(14)
W(8)-O(33)	1.899(11)	W(6)-O(18)	1.918(11)	W(14)-O(57)	1.878(15)
W(8)-O(36)	1.914(12)	W(6)-O(16)	1.942(11)	W(14)-O(52)	1.884(13)
W(8)-O(48)	1.919(11)	W(6)-O(3)	2.342(9)	W(14)-O(66)^{i}	2.34(2)
W(8)-O(10)	1.921(11)	W(7)-O(30)	1.660(12)	W(14)-O(64)^{i}	2.43(2)
W(8)-O(7)	2.368(11)	W(7)-O(17)	1.890(10)	W(15)-O(1)	1.633(13)
W(9)-O(23)	1.679(11)	W(7)-O(12)	1.898(11)	W(15)-O(59B)	1.74(2)
W(9)-O(21)	1.883(11)	W(7)-O(34)	1.912(12)	W(15)-O(57)	1.886(16)
W(16)-O(56)	1.886(17)	W(7)-O(42)	1.951(11)	W(15)-O(63)	1.906(16)
W(16)-O(61)	1.915(15)	W(7)-O(26)	2.361(11)	W(15)-O(54)	1.910(15)
W(16)-O(65A)	1.83(2)	W(15)-O(66)^{i}	2.44(2)	W(15)-O(59A)	2.12(3)
W(16)-O(63)	1.882(17)	W(16)-O(39)	1.710(11)	W(15)-O(55)	2.41(2)
W(1)-O(37)	1.692(12)	W(9)-O(5)	1.895(10)	W(16)-O(65B)	2.02(3)
W(1)-O(12)	1.897(11)	W(9)-O(18)	1.931(10)	W(16)-O(55)	2.37(2)
W(1)-O(28)	1.906(11)	W(9)-O(36)	1.936(12)	W(16)-O(58)	2.43(2)
W(1)-O(25)	1.910(10)	W(9)-O(3)	2.375(10)	W(17)-O(40)	1.658(14)
W(1)-O(21)	1.921(11)	W(10)-O(45)	1.675(13)	W(17)-O(61)^{i}	1.873(14)
W(1)-O(3)	2.383(10)	W(10)-O(53)	1.861(14)	W(17)-O(51)	1.886(14)
W(2)-O(44)	1.703(13)	W(10)-O(59B)	1.89(2)	W(17)-O(53)	1.911(13)
W(2)-O(10)	1.867(11)	W(10)-O(56)	1.903(17)	W(17)-O(62)	1.928(17)
W(2)-O(5)	1.914(11)	W(10)-O(52)^{i}	1.916(15)	W(17)-O(58)^{i}	2.34(2)
W(2)-O(32)	1.917(11)	W(10)-O(59A)	1.96(2)	W(17)-O(64)	2.47(2)
W(2)-O(8)	1.919(12)	W(10)-O(55)	2.33(2)	W(18)-O(2)	1.689(15)
W(2)-O(4)	2.357(11)	W(10)-O(64)	2.406(19)	W(18)-O(62)	1.845(17)
W(3)-O(20)	1.696(11)	W(11)-O(27)	1.714(11)	W(18)-O(65A)^{i}	1.87(2)
W(3)-O(34)	1.865(12)	W(11)-O(16)	1.894(11)	W(18)-O(54)	1.866(14)
W(3)-O(13)	1.922(11)	W(11)-O(42)	1.917(12)	W(18)-O(60)	1.917(16)
W(3)-O(24)	1.926(12)	W(11)-O(14)	1.941(11)	W(18)-O(65B)^{i}	2.04(3)
W(3)-O(14)	1.936(10)	W(11)-O(43)	1.947(13)	W(18)-O(66)^{i}	2.37(2)
W(3)-O(26)	2.335(11)	W(11)-O(26)	2.336(10)	W(18)-O(58)^{i}	2.40(2)

W(4)-O(15)	1.718(12)	W(12)-O(49)	1.687(11)	Si(1)-O(64)	1.56(2)
W(4)-O(24)	1.895(12)	W(12)-O(43)	1.902(13)	Si(1)-O(64)^{i}	1.56(2)
W(4)-O(6)	1.904(10)	W(12)-O(41)	1.908(12)	Si(1)-O(58)	1.62(2)
W(4)-O(33)	1.912(13)	W(12)-O(48)	1.916(13)	Si(1)-O(58)^{i}	1.62(2)
W(4)-O(41)	1.940(10)	W(12)-O(9)	1.929(11)	Si(1)-O(66)	1.65(2)
W(4)-O(7)	2.284(11)	W(12)-O(7)	2.358(10)	Si(1)-O(66)^{i}	1.65(2)
W(5)-O(38)	1.696(11)	W(13)-O(46)	1.690(12)	Si(1)-O(55)^{i}	1.657(18)
W(5)-O(28)	1.900(11)	W(13)-O(13)	1.885(11)	Si(1)-O(55)	1.657(18)
W(5)-O(17)	1.912(10)	W(13)-O(32)	1.917(11)	Si(2)-O(3)	1.606(11)
W(5)-O(29)	1.927(12)	W(13)-O(6)	1.917(11)	Si(2)-O(4)	1.618(10)
W(5)-O(8)	1.960(12)	W(13)-O(29)	1.930(11)	Si(2)-O(7)	1.625(11)
W(5)-O(4)	2.359(10)	W(13)-O(4)	2.353(11)	Si(2)-O(26)	1.629(12)
W(6)-O(11)	1.735(10)	W(14)-O(50)	1.651(14)	W(14)-O(60)	1.859(16)
W(6)-O(9)	1.882(11)				

O(31)-Sm(1)-O(19)	97.2(4)	O(5W)-Sm(1)-N(5)	124.0(4)	O(3W)-Sm(2)-O(2W)	82.1(5)
O(31)-Sm(1)-O(1W)	75.4(4)	O(4W)-Sm(1)-N(5)	123.8(4)	O(39)-Sm(2)-O(2W)	69.6(5)
O(19)-Sm(1)-O(1W)	74.6(4)	O(11)-Sm(1)-N(5)	69.4(4)	O(35)-Sm(2)-O(2W)	74.5(4)
O(31)-Sm(1)-O(5W)	141.0(4)	N(4)-Sm(1)-N(5)	60.1(4)	O(22)-Sm(2)-N(10)	153.0(5)
O(19)-Sm(1)-O(5W)	90.8(4)	O(31)-Sm(1)-N(3)	147.7(4)	O(15)-Sm(2)-N(10)	77.0(4)
O(1W)-Sm(1)-O(5W)	143.0(4)	O(19)-Sm(1)-N(3)	62.8(4)	O(3W)-Sm(2)-N(10)	114.3(5)
O(31)-Sm(1)-O(4W)	71.8(4)	O(1W)-Sm(1)-N(3)	74.8(4)	O(39)-Sm(2)-N(10)	68.9(4)
O(19)-Sm(1)-O(4W)	72.5(4)	O(5W)-Sm(1)-N(3)	68.3(4)	O(35)-Sm(2)-N(10)	61.7(4)
O(1W)-Sm(1)-O(4W)	129.3(4)	O(4W)-Sm(1)-N(3)	119.8(5)	O(2W)-Sm(2)-N(10)	125.1(4)
O(5W)-Sm(1)-O(4W)	74.6(5)	O(11)-Sm(1)-N(3)	125.2(4)	O(22)-Sm(2)-N(12)	62.3(4)
O(31)-Sm(1)-O(11)	86.1(4)	N(4)-Sm(1)-N(3)	61.3(4)	O(15)-Sm(2)-N(12)	73.5(4)
O(19)-Sm(1)-O(11)	144.2(4)	N(5)-Sm(1)-N(3)	116.2(4)	O(3W)-Sm(2)-N(12)	71.8(4)
O(1W)-Sm(1)-O(11)	139.7(4)	O(22)-Sm(2)-O(15)	76.6(4)	O(39)-Sm(2)-N(12)	138.2(5)
O(5W)-Sm(1)-O(11)	66.4(4)	O(22)-Sm(2)-O(3W)	90.8(5)	O(35)-Sm(2)-N(12)	144.7(4)
O(4W)-Sm(1)-O(11)	74.9(4)	O(15)-Sm(2)-O(3W)	145.1(4)	O(2W)-Sm(2)-N(12)	120.2(5)
O(31)-Sm(1)-N(4)	123.1(4)	O(22)-Sm(2)-O(39)	133.0(4)	N(10)-Sm(2)-N(12)	114.6(4)
O(19)-Sm(1)-N(4)	122.0(4)	O(15)-Sm(2)-O(39)	141.0(4)	O(22)-Sm(2)-N(11)	121.0(4)
O(1W)-Sm(1)-N(4)	77.5(5)	O(3W)-Sm(2)-O(39)	69.7(4)	O(15)-Sm(2)-N(11)	80.6(4)
O(5W)-Sm(1)-N(4)	82.3(5)	O(22)-Sm(2)-O(35)	104.2(4)	O(3W)-Sm(2)-N(11)	78.4(5)
O(4W)-Sm(1)-N(4)	153.2(4)	O(15)-Sm(2)-O(35)	71.6(4)	O(39)-Sm(2)-N(11)	97.2(4)
O(11)-Sm(1)-N(4)	83.6(4)	O(3W)-Sm(2)-O(35)	143.3(4)	O(35)-Sm(2)-N(11)	118.6(4)
O(31)-Sm(1)-N(5)	64.0(4)	O(39)-Sm(2)-O(35)	75.8(4)	O(2W)-Sm(2)-N(11)	159.4(5)
O(19)-Sm(1)-N(5)	143.3(4)	O(22)-Sm(2)-O(2W)	65.5(4)	N(10)-Sm(2)-N(11)	59.2(4)
O(1W)-Sm(1)-N(5)	70.3(4)	O(15)-Sm(2)-O(2W)	119.8(5)	N(12)-Sm(2)-N(11)	59.3(4)

Symmetry codes: (i) -x+2, -y+3, -z+1.

Table S3. The selected bond lengths (Å) and bond angles (°) for **2Eu**.

Eu(1)-O(31)	2.377(10)	Eu(1)-N(4)	2.553(13)	Eu(2)-O(35)	2.436(10)
Eu(1)-O(19)	2.421(9)	Eu(1)-N(3)	2.558(12)	Eu(2)-O(39)	2.445(9)
Eu(1)-O(1W)	2.426(11)	Eu(1)-N(5)	2.562(12)	Eu(2)-O(2W)	2.473(12)
Eu(1)-O(4W)	2.442(12)	Eu(2)-O(22)	2.374(10)	Eu(2)-N(10)	2.568(13)
Eu(1)-O(5W)	2.470(10)	Eu(2)-O(15)	2.393(10)	Eu(2)-N(12)	2.599(13)
Eu(1)-O(11)	2.491(9)	Eu(2)-O(3W)	2.401(12)	Eu(2)-N(11)	2.609(12)
O(31)-Eu(1)-O(19)	96.5(3)	O(4W)-Eu(1)-N(3)	118.9(4)	O(3W)-Eu(2)-O(2W)	81.1(5)
O(31)-Eu(1)-O(1W)	75.2(4)	O(5W)-Eu(1)-N(3)	68.7(4)	O(35)-Eu(2)-O(2W)	74.2(4)
O(19)-Eu(1)-O(1W)	74.0(4)	O(11)-Eu(1)-N(3)	126.3(4)	O(39)-Eu(2)-O(2W)	70.0(4)
O(31)-Eu(1)-O(4W)	72.7(4)	N(4)-Eu(1)-N(3)	61.7(4)	O(22)-Eu(2)-N(10)	152.9(4)
O(19)-Eu(1)-O(4W)	71.8(4)	O(31)-Eu(1)-N(5)	63.6(4)	O(15)-Eu(2)-N(10)	76.4(4)
O(1W)-Eu(1)-O(4W)	129.2(4)	O(19)-Eu(1)-N(5)	143.5(4)	O(3W)-Eu(2)-N(10)	115.7(4)
O(31)-Eu(1)-O(5W)	141.0(4)	O(1W)-Eu(1)-N(5)	71.4(4)	O(35)-Eu(2)-N(10)	63.6(4)
O(19)-Eu(1)-O(5W)	92.3(4)	O(4W)-Eu(1)-N(5)	123.8(4)	O(39)-Eu(2)-N(10)	69.4(4)
O(1W)-Eu(1)-O(5W)	143.4(4)	O(5W)-Eu(1)-N(5)	122.8(4)	O(2W)-Eu(2)-N(10)	126.1(4)
O(4W)-Eu(1)-O(5W)	74.3(4)	O(11)-Eu(1)-N(5)	69.0(3)	O(22)-Eu(2)-N(12)	62.3(4)
O(31)-Eu(1)-O(11)	85.4(3)	N(4)-Eu(1)-N(5)	60.5(4)	O(15)-Eu(2)-N(12)	72.9(4)
O(19)-Eu(1)-O(11)	143.5(4)	N(3)-Eu(1)-N(5)	117.0(4)	O(3W)-Eu(2)-N(12)	71.4(4)
O(1W)-Eu(1)-O(11)	140.4(4)	O(22)-Eu(2)-O(15)	77.2(4)	O(35)-Eu(2)-N(12)	143.5(4)
O(4W)-Eu(1)-O(11)	74.1(4)	O(22)-Eu(2)-O(3W)	89.4(4)	O(39)-Eu(2)-N(12)	138.0(4)
O(5W)-Eu(1)-O(11)	66.0(3)	O(15)-Eu(2)-O(3W)	144.1(4)	O(2W)-Eu(2)-N(12)	119.7(4)
O(31)-Eu(1)-N(4)	123.1(4)	O(22)-Eu(2)-O(35)	102.4(4)	N(10)-Eu(2)-N(12)	114.1(4)
O(19)-Eu(1)-N(4)	122.9(4)	O(15)-Eu(2)-O(35)	71.3(3)	O(22)-Eu(2)-N(11)	121.6(4)
O(1W)-Eu(1)-N(4)	78.4(4)	O(3W)-Eu(2)-O(35)	144.5(4)	O(15)-Eu(2)-N(11)	80.1(4)
O(4W)-Eu(1)-N(4)	152.4(4)	O(22)-Eu(2)-O(39)	132.8(3)	O(3W)-Eu(2)-N(11)	79.1(4)
O(5W)-Eu(1)-N(4)	81.4(4)	O(15)-Eu(2)-O(39)	141.3(4)	O(35)-Eu(2)-N(11)	119.6(4)
O(11)-Eu(1)-N(4)	84.2(4)	O(3W)-Eu(2)-O(39)	70.3(4)	O(39)-Eu(2)-N(11)	96.5(4)
O(31)-Eu(1)-N(3)	147.5(4)	O(35)-Eu(2)-O(39)	77.5(4)	O(2W)-Eu(2)-N(11)	159.0(4)
O(19)-Eu(1)-N(3)	63.2(4)	O(22)-Eu(2)-O(2W)	65.0(4)	N(10)-Eu(2)-N(11)	58.5(4)
O(1W)-Eu(1)-N(3)	74.8(4)	O(15)-Eu(2)-O(2W)	120.6(4)	N(12)-Eu(2)-N(11)	59.8(4)

Table S4. The selected bond lengths (Å) and bond angles (°) for **3Tb**.

Tb(1)-O(31)	2.325(13)	Tb(1)-N(4)	2.534(18)	Tb(2)-O(35)	2.402(14)
Tb(1)-O(1W)	2.393(16)	Tb(1)-N(5)	2.538(17)	Tb(2)-O(39)	2.434(12)
Tb(1)-O(19)	2.403(14)	Tb(1)-N(3)	2.545(16)	Tb(2)-O(2W)	2.461(16)
Tb(1)-O(5W)	2.412(15)	Tb(2)-O(22)	2.350(14)	Tb(2)-N(10)	2.571(17)
Tb(1)-O(4W)	2.424(15)	Tb(2)-O(3W)	2.373(15)	Tb(2)-N(11)	2.601(17)
Tb(1)-O(11)	2.501(12)	Tb(2)-O(15)	2.385(13)	Tb(2)-N(12)	2.604(16)
O(31)-Tb(1)-O(1W)	75.2(5)	O(5W)-Tb(1)-N(5)	122.8(5)	O(15)-Tb(2)-O(2W)	121.6(5)
O(31)-Tb(1)-O(19)	95.7(5)	O(4W)-Tb(1)-N(5)	123.6(5)	O(35)-Tb(2)-O(2W)	75.0(5)
O(1W)-Tb(1)-O(19)	74.6(5)	O(11)-Tb(1)-N(5)	69.4(5)	O(39)-Tb(2)-O(2W)	70.6(5)
O(31)-Tb(1)-O(5W)	140.6(5)	N(4)-Tb(1)-N(5)	61.6(6)	O(22)-Tb(2)-N(10)	151.5(5)
O(1W)-Tb(1)-O(5W)	143.7(5)	O(31)-Tb(1)-N(3)	147.4(5)	O(3W)-Tb(2)-N(10)	116.1(6)
O(19)-Tb(1)-O(5W)	92.1(5)	O(1W)-Tb(1)-N(3)	75.2(5)	O(15)-Tb(2)-N(10)	75.6(5)
O(31)-Tb(1)-O(4W)	71.9(5)	O(19)-Tb(1)-N(3)	63.3(5)	O(35)-Tb(2)-N(10)	62.6(5)
O(1W)-Tb(1)-O(4W)	129.2(5)	O(5W)-Tb(1)-N(3)	68.7(5)	O(39)-Tb(2)-N(10)	68.4(5)
O(19)-Tb(1)-O(4W)	71.4(5)	O(4W)-Tb(1)-N(3)	118.6(6)	O(2W)-Tb(2)-N(10)	125.8(5)
O(5W)-Tb(1)-O(4W)	74.2(6)	O(11)-Tb(1)-N(3)	126.0(5)	O(22)-Tb(2)-N(11)	121.9(5)
O(31)-Tb(1)-O(11)	86.0(5)	N(4)-Tb(1)-N(3)	61.0(5)	O(3W)-Tb(2)-N(11)	77.6(6)
O(1W)-Tb(1)-O(11)	140.6(5)	N(5)-Tb(1)-N(3)	117.5(5)	O(15)-Tb(2)-N(11)	80.7(5)
O(19)-Tb(1)-O(11)	142.7(5)	O(22)-Tb(2)-O(3W)	90.8(6)	O(35)-Tb(2)-N(11)	120.7(5)
O(5W)-Tb(1)-O(11)	65.4(5)	O(22)-Tb(2)-O(15)	76.9(5)	O(39)-Tb(2)-N(11)	95.5(5)
O(4W)-Tb(1)-O(11)	73.8(5)	O(3W)-Tb(2)-O(15)	144.1(5)	O(2W)-Tb(2)-N(11)	157.2(6)
O(31)-Tb(1)-N(4)	125.0(5)	O(22)-Tb(2)-O(35)	101.4(5)	N(10)-Tb(2)-N(11)	60.2(5)
O(1W)-Tb(1)-N(4)	78.6(6)	O(3W)-Tb(2)-O(35)	144.6(5)	O(22)-Tb(2)-N(12)	62.9(5)
O(19)-Tb(1)-N(4)	122.4(5)	O(15)-Tb(2)-O(35)	71.2(5)	O(3W)-Tb(2)-N(12)	70.7(5)
O(5W)-Tb(1)-N(4)	80.8(6)	O(22)-Tb(2)-O(39)	134.0(5)	O(15)-Tb(2)-N(12)	73.7(5)
O(4W)-Tb(1)-N(4)	152.1(6)	O(3W)-Tb(2)-O(39)	70.7(5)	O(35)-Tb(2)-N(12)	144.1(5)
O(11)-Tb(1)-N(4)	84.7(5)	O(15)-Tb(2)-O(39)	140.1(5)	O(39)-Tb(2)-N(12)	137.6(5)
O(31)-Tb(1)-N(5)	64.4(5)	O(35)-Tb(2)-O(39)	77.2(5)	O(2W)-Tb(2)-N(12)	118.9(5)
O(1W)-Tb(1)-N(5)	71.3(6)	O(22)-Tb(2)-O(2W)	64.9(5)	N(10)-Tb(2)-N(12)	115.3(5)
O(19)-Tb(1)-N(5)	143.8(5)	O(3W)-Tb(2)-O(2W)	80.6(6)	N(11)-Tb(2)-N(12)	59.5(5)

Table S5. Hydrogen bonds for **1Sm** [Å and °].

D—H···*A*	*D*—H	H···*A*	*D*···*A*	*D*—H···*A*
N1—H1*A*···O35^{i}	0.86	2.08	2.94 (2)	177
N1—H1*B*···O20^{i}	0.86	2.49	3.18 (2)	137
N1—H1*B*···O23^{ii}	0.86	2.45	3.22 (2)	148
N2—H2*A*···O20^{i}	0.86	2.26	2.93 (2)	135
N6—H6*B*···O14^{iii}	0.86	2.30	3.05 (2)	147
N7—H7*A*···O7*W*^{iii}	0.86	2.23	2.98 (2)	145
N7—H7*B*···O14^{iii}	0.86	2.48	3.24 (2)	147
N7—H7*B*···O43^{iii}	0.86	2.57	3.09 (2)	120
N8—H8*A*···O19^{iv}	0.86	2.17	2.97 (2)	155
N8—H8*B*···O8*W*^{v}	0.86	2.34	3.12 (2)	150
N9—H9*A*···O8*W*^{v}	0.86	2.22	3.01 (2)	152
N13—H13*A*···O7*W*	0.86	2.20	2.95 (2)	145
N14—H14*A*···O36^{vi}	0.86	2.26	3.08 (2)	159
C6—H6*A*···O38^{vii}	0.93	2.33	3.21 (2)	158
C10—H10*A*···O38^{vii}	0.96	2.52	3.40 (2)	153
C11—H11*B*···O28^{ii}	0.96	2.27	3.22 (2)	168
C15—H15*A*···O45^{iii}	0.93	2.54	3.45 (3)	166
C21—H21*C*···O53^{viii}	0.96	2.35	3.21 (3)	148
C22—H22*A*···O45^{iii}	0.96	2.42	3.27 (3)	147
C22—H22*B*···O40^{ix}	0.97	2.59	3.54 (3)	166

Symmetry codes: (i) *x*−1, *y*+1, *z*; (ii) *x*, *y*+1, *z*; (iii) *x*−1, *y*, *z*; (iv) *x*+1, *y*−1, *z*; (v) −*x*+1, −*y*+3, −*z*+1; (vi) *x*+1, *y*, *z*; (vii) −*x*, −*y*+4, −*z*+2; (viii) 2−*x*, −*y*+4, −*z*+1; (ix) 2−*x*, −*y*+3, −*z*+1.

Table S6. Hydrogen bonds for **2Eu** [Å and °].

D—H···*A*	*D*—H	H···*A*	*D*···*A*	*D*—H···*A*
N1—H1*A*···O35^{i}	0.86	2.06	2.92 (2)	174
N1—H1*B*···O20^{i}	0.86	2.52	3.19 (2)	135
N1—H1*B*···O23^{ii}	0.86	2.44	3.21 (2)	150
N2—H2*A*···O20^{i}	0.86	2.24	2.93 (2)	137
N6—H6*B*···O14^{iii}	0.86	2.26	3.01 (2)	146
N7—H7*A*···O7*W*^{iii}	0.86	2.25	3.00 (2)	144
N7—H7*B*···O14^{iii}	0.86	2.39	3.16 (2)	149
N8—H8*A*···O19^{iv}	0.86	2.10	2.93 (2)	162
N8—H8*B*···O8*W*^{v}	0.86	2.41	3.16 (2)	146
N9—H9*A*···O8*W*^{v}	0.86	2.19	2.96 (2)	150
N13—H13*A*···O7*W*	0.86	2.18	2.94 (2)	148
N14—H14*A*···O36^{vi}	0.86	2.27	3.10 (2)	160
C6—H6*A*···O38^{vii}	0.93	2.33	3.25 (2)	170
C10—H10*A*···O38^{vii}	0.96	2.48	3.38 (2)	156
C10—H10*C*···O37	0.96	2.59	3.39 (2)	140
C11—H11*B*···O28^{ii}	0.96	2.28	3.23 (2)	171
C15—H15*A*···O45^{iii}	0.93	2.45	3.37 (2)	170
C21—H21*C*···O53^{viii}	0.96	2.45	3.26 (3)	142
C22—H22*A*···O45^{iii}	0.96	2.35	3.23 (3)	152
C22—H22*B*···O40^{ix}	0.97	2.57	3.50 (3)	166

Symmetry codes: (i) *x*−1, *y*+1, *z*; (ii) *x*, *y*+1, *z*; (iii) *x*−1, *y*, *z*; (iv) *x*+1, *y*−1, *z*; (v) −*x*+1, −*y*+3, −*z*+1; (vi) *x*+1, *y*, *z*; (vii) −*x*, −*y*+4, −*z*+2; (viii) 2−*x*, −*y*+4, −*z*+1; (ix) 2−*x*, −*y*+3, −*z*+1.

Table S7. Hydrogen bonds for **3Tb** [Å and °].

D—H···*A*	*D*—H	H···*A*	*D*···*A*	*D*—H···*A*
N1—H1*A*···O35^{i}	0.86	2.1	2.95(2)	172
N1—H1*B*···O20^{i}	0.86	2.53	3.19(2)	135
N1—H1*B*···O23^{ii}	0.86	2.48	3.26(2)	152
N2—H2*A*···O20^{i}	0.86	2.23	2.92(2)	138
N6—H6*B*···O14^{iii}	0.86	2.31	3.07(2)	146
N7—H7*A*···O7*W*^{iii}	0.86	2.17	2.95(3)	152
N7—H7*B*···O14^{iii}	0.86	2.47	3.23(2)	147
N8—H8*A*···O19^{iv}	0.86	2.13	2.96(2)	161
N8—H8*B*···O8*W*^{v}	0.86	2.39	3.16(3)	149
N9—H9*A*···O8*W*^{v}	0.86	2.18	2.98(3)	154
N13—H13*A*···O7*W*	0.86	2.16	2.93(3)	149
N14—H14*A*···O36^{vi}	0.86	2.28	3.12(2)	165
C6—H6*A*···O38^{vii}	0.93	2.31	3.20(3)	159
C10—H10*A*···O38^{vii}	0.96	2.52	3.40(3)	153
C11—H11*B*···O28^{ii}	0.96	2.27	3.21(3)	170
C15—H15*A*···O45^{iii}	0.93	2.5	3.42(3)	174
C21—H21*C*···O53^{viii}	0.96	2.42	3.23(3)	142
C22—H22*A*···O45^{iii}	0.96	2.32	3.22(4)	156
C22—H22*B*···O40^{ix}	0.97	2.52	3.48(3)	172

Symmetry codes: (i) *x*−1, *y*+1, *z*; (ii) *x*, *y*+1, *z*; (iii) *x*−1, *y*, *z*; (iv) *x*+1, *y*−1, *z*; (v) −*x*+1, −*y*+3, −*z*+1; (vi) *x*+1, *y*, *z*; (vii) −*x*, −*y*+4, −*z*+2; (viii) 2−*x*, −*y*+4, −*z*+1; (ix) 2−*x*, −*y*+3, −*z*+1.

Table 8. The third-order NLO data of some POMs-based compounds.

Compounds	β^a (cm·GM^{-1})	σ^b (GM)	λ (nm)	ref
1Sm	0.021047	1383	680	This work
2Eu	0.013874	669	700	This work
3Tb	0.011443	712	720	This work
$[(L\text{-}C_4O_6H_2)_2V_4O_8]\cdot 2C_6N_2H_{18}$	0.003167	1412	740	1
$[(D\text{-}C_4O_6H_2)_2V_4O_8]\cdot 2C_6N_2H_{18}$	0.003167	1094	740	1
$[Co(H_2O)_2(DAPSC)]_3\{[Co(H_2O)(DAPSC)]_2BW_{12}O_{40}\}BW_{12}O_{40}\cdot 10H_2O$	0.003553	1522	720	2
$[Zn(H_2O)_2(DAPSC)]_3\{[Zn(H_2O)(DAPSC)]_2BW_{12}O_{40}\}BW_{12}O_{40}\cdot 8H_2O$	0.005132	2199	720	2
$Na_2[(CH_3)_2NH_2]_3\{Na\subset[Ce^{III}(H_2O)(CH_3CH_2OH)(L\text{-}tartH_3)(H_2Si_2W_{19}O_{66})]\}\cdot 3.5H_2O$	0.01369	389	740	3
$[(CH_3)_2NH_2]_7\{Na\subset[Ce^{III}(H_2O)(CH_3CH_2OH)(D\text{-}tartH_3)(Si_2W_{19}O_{66})]\}\cdot 2.5H_2O$	0.00279	392	740	3
$[Mn(H_2O)_2(DAPSC)]_2\{[Na_3(H_2O)_2Mn_{0.5}(H_2O)_4][Mn(H_2O)(DAPSC)]_2[H_3P_5W_{30}O_{110}]\}\cdot 7.5H_2O$	0.002099	888	-	4
$[Co(H_2O)_2(DAPSC)]\{[Co(H_2O)_2(DAPSC)][Na_{1.5}(H_2O)_2]\}\{[Na_{0.5}(H_2O)_2Co_{0.5}(H_2O)_4][Co(H_2O)(DAPSC)]_2[H_4P_5W_{30}O_{110}]\}\cdot 6H_2O$	0.001715	707	-	4
$[Ni(NTB)(H_2O)]_2(H_2P_2Mo_5O_{23})\cdot 9.25H_2O$	0.001655	758	720	5
$[Ni(H_2O)(NTB)]_2(PMo^{VI}_{11}MoVO_{40})\cdot 4.5H_2O$	0.001127	404	920	5
$[Ni(NTB)]_2(Mo_8O_{26})\cdot 9H_2O$	0.015925	673	780	5
$[Co(H_2O)_6]\{[C_3H_4N_2]_2[C_5NH_5]_{14}[H_{15}(Mo_2O_4)_8Co_{16}(PO_4)_{14}(HPO_3)_{10}(OH)_3]\}\cdot 5H_2O$	0.01375	622	730	6
$[C_3H_5N_2]_4[C_5NH_5]_2[Ni(H_2O)_6]\{[C_3H_4N_2]_2[C_5NH_5]_{14}[H_{18}(Mo_2O_4)_8Ni_{16}(PO_4)_{22}(OH)_6]\}\cdot 11H_2O$	0.0056	274	750	6
$[C_5NH_5]_8[C_3H_5N_2]_2\{[C_5NH_5]_9[H_{31}Mo_{12}O_{24}Co_{12}(PO_4)_{23}(H_2O)_4]\}\cdot 12H_2O$	0.00263	1058	820	7

[a] TPA absorption coefficient of the solution. [b] molecular TPA cross-section.

REFERENCES

(1) Cao, J.; Xiong, Y.; Luo, X.; Chen, L.; Shi, J.; Zhou, M.; Xu, Y. A pair of new chiral polyoxovanadates with decent NLO properties. *Dalton Trans.* **2018**, *47*, 6054-6058.

(2) Hu, G. H.; Miao, H.; Mei, H.; Zhou, S.; Xu, Y. Two novel bi-functional hybrid materials constructed from POMs and a Schiff base with excellent third-order NLO and catalytic properties. *Dalton Trans.* **2016**, *45*, 7947-7951.

(3) Ju, W.-W.; Zhang, H.-T.; Xu, X.; Zhang, Y.; Xu, Y. Enantiomerically Pure Lanthanide−Organic Polytungstates Exhibiting Two-Photon Absorption Properties. *Inorg. Chem.* **2014**, *53*, 3269-3271.

(4) Shi, J.; Xiong, Y.; Zhou, M; Chen, L.;Xu, Y. Two hybrid polyoxometalates constructed from Preyssler P_5W_{30} clusters and Schiff base exhibiting interesting third-order NLO properties. *RSC Adv.* **2017**, *7*, 55427-55433.

(5) Dong, Y. Y.; Xu, X.; Zhou, G. P.; Miao, H.; Hu, G. H.; Xu, Y. Three novel polyoxoanion-supported compounds: confinement of polyoxoanions in Ni-containing rigid concave surfaces with enhanced NLO properties. *Dalton Trans.* **2015**, *44*, 18347-18353.
(6) Miao, H.; Wan, H. X.; Liu, M.; Zhang, Y.; Xu, X.; Ju, W. W.; Zhu, D. R.; Xu, Y. Two novel organic-inorganic hybrid molybdenum (V) cobalt/nickel phosphate compounds based on isolated nanosized Mo/Co(Ni)/P cluster wheels. *J. Mater. Chem. C* **2014**, *2*, 6554-6560.
(7) Dong, Y. Y.; Hu, G. H.; Miao, H.; He, X. X.; Fang, M.; Xu, Y. An Unprecedented M–O Cluster Constructed from Nanosized $\{[C_5NH_5]_9[H_{31}Mo^{V}_{12}O_{24}Co^{II}_{12}(PO_4)_{23}(H_2O)_4]\}^{2-}$ Anions Exhibiting Interesting Nonlinear-Optical Properties. *Inorg. Chem.* **2016**, *55*, 11621-11625.